

How to Cite:

Jayaprakash, P., Srinivasan, K., & Das, D. (2022). Application of synthetic jet actuator to delay the flow separation in symmetrical airfoil. *International Journal of Health Sciences*, 6(S5), 3712–3727. <https://doi.org/10.53730/ijhs.v6nS5.9405>

Application of synthetic jet actuator to delay the flow separation in symmetrical airfoil

Jayaprakash P

Assistant Professor, Department of Aeronautical Engineering, Dhanalakshmi Srinivasan College Of Engineering & Technology – Mamallapuram
Email: prakashair11@gmail.com

K. Srinivasan

Assistant Professor, Department of Mechanical Engineering, Dhanalakshmi Srinivasan College Of Engineering & Technology – Mamallapuram
Email: srinivasank.mech@dscet.ac.in

Durlab Das

Assistant Professor, Department of Aeronautical Engineering, Dhanalakshmi Srinivasan College Of Engineering & Technology – Mamallapuram
Email: durlab1993@gmail.com

Abstract--The objective of this project is to delay the flow separation over the symmetrical airfoil by placing the synthetic jet actuator. A synthetic jet actuator is a device which moves a fluid in and outside a cavity through a small orifice and also it will maximize the aerodynamic performance of the airfoil. The aerodynamic characteristic of the airfoil have been compared in detail at different angles of attack, for the case with and without adoption of synthetic jet. This control device is having zero mass flux active flow control device. The external flow around the airfoil will be determined by using numerical approach. By changing the angle of attack we can analyse how the separation of flows are varied. Results of this study demonstrated the actuator effectiveness on overall aerodynamic performance and show consistent trends with high-order Computational Fluid Dynamics (CFD).

Keywords--Computational Fluid Dynamics, airfoil, aerodynamic.

Introduction

Synthetic jet (SJ) technology is also called as zero-mass jet technology because it does not require extra energy injection. The net mass flux has been zero since the air surrounding the jet orifice is sucked and blown periodically. The synthetic jet

generates momentum difference that change the behaviour of the flow. Figure 1.1 shows the most common practical form of the actuator with the output perpendicular to the stream. At present, this technology has been widely used in various engineering field. In 1998, Smith and Glezer developed successfully a synthetic jet actuator (SJ) and also proved that the interaction of the jet with the flow over the surface can displace the local streamlines and induce a virtual change in the shape of the surface. The jet actuator consist of a metal diaphragm, piezoelectric material, a cavity and a jet hole. Piezoelectric materials produce a periodic motion of the metal diaphragm and compress the volume of the cavity, and the periodic suction will be formed at the orifice of the jet. The gas will form a vortex pair during this continuous suction process, which will mix the low-velocity fluid in the bottom layer of the boundary layer with the high-energy fluid in the mainstream. The energy at the bottom of the boundary layer is strengthened, thus reducing the pressure gradient and delaying the flow separation phenomenon.

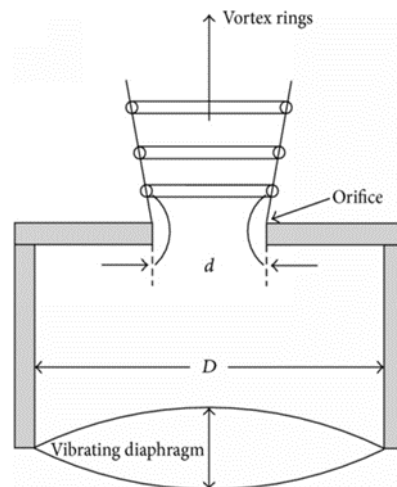


Figure.1.1 Synthetic Jet Actuator

In 2005, Holman et al. mentioned one of the synthetic jet actuator's ability. It has the ability to integrate the internal flow of the cavity with the external flow without an external device. This makes it an attractive device for flow control in both internal and external flows. Moreover, Ritchie et al. demonstrate that the synthetic jet actuators have the advantage of a greater spreading rate than that of the equivalent continuous jet throughout the measured domain at the same time-averaged velocity, thus yielding a greater region of influence on the working domain.

The jet stream can be simulated like a stream with complex spartial and temporal charateristics, Flow typically separates from the edge of the slot and a vortex sheet is formed, which rotated as single and isolated vortices, and subsequently being driven by self induced velocity. Eventually, the vortices lose their coherence and disappear as they move away from the orifice. The vortices that are created never return to the orifice at suction time, if the synthetic jet can generate the strong velocity. Recent experimental and numerical studies are testifying that use

of synthetic jet actuator as a flow control device is desirable. However, there is still a limited amount of this type of flow control devices that are used on aircraft structures. In recent years, the numerical simulation of the synthetic jets used for stall control around an aerodynamic body has attracted the attention of many researchers. This popularity might be because numerical simulation is a very effective way to explore the possibilities of using synthetic jet on an aircraft. In order to simulate flow control with the synthetic jet, Large eddy simulation method (LES) and Direct Numerical solution method (DNS) for resolving small vortices induced by synthetic jet as they are very convenient. Simulation of the flow high Reynolds number is unfeasible because of high computational cost and difficulties in the simulation. In fact, most numerical simulation for stall control with the presence of the synthetic jet were performed using Reynolds average Navier- stokes equations method.

In recent year, with the development of micro-electromechanical technology, SJ technology has been developed rapidly. Some work has been conducted to investigate the mechanism of jet. Seifert et al applied the jet actuator to an airfoil, and the aerodynamic performance of the airfoil was improved obviously. Qin et al used end wall SJ to control the flow separation of stator cascade of high-load compressor. The result showed that the end wall SJ can significantly improve the flow in the blade channel. Under the design condition, the maximum loss is reduced by 21.63 and the pressure increment is 5.6%.

Experimentally studied the flow separation and stall control of NACA 0012 airfoil at different angle of attack using a high-energy jet actuator. The results showed that the lift curve increased with increasing excitation frequency at small angle of attack. Under the excitation control of SJA, the stalling angle of attack increased from 12° to 18° . Zhao et al examined numerically the effects of jet control parameters on the dynamic stall characteristics of the OA212 rotor aerofoil.

All the mentioned work has contributed to the understanding and application of SJ on flow control. However, the comprehensive analysis and optimal design of main parameters affecting the control effect of the jet still need to be further investigated.

This project work deals with the simulation of the synthetic jet actuator located on the section surface of a NACA0012 airfoil as an active flow controller. Unsteady flow over a NACA0012 airfoil is solved using a Navier- stokes this solver. The parametric study demonstrates the synthetic jet parameters must be optimized for improving aerodynamic performance. To the best of authors' knowledge, in literatures, there is no available work dealing with optimization of the jet location, jet frequency and the slot size. The objective of this project is to determine those synthetic jet parameters that maximize the L/D ratio.

1.1 Airfoil Nomenclature

An airfoil is the cross-sectional shape of a wing. An airfoil-shaped body moved through a fluid produces an aerodynamic force.

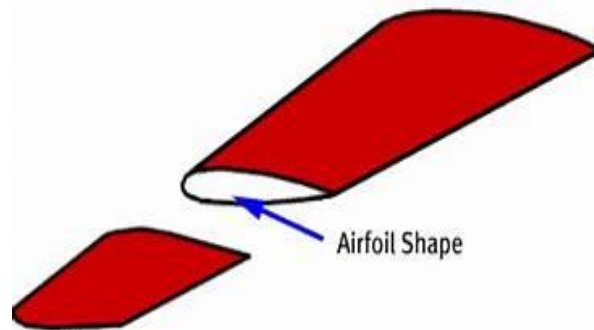


Figure.1.2 Cross section of airfoil

1.1.1 Terminology

- The suction surface (upper surface) is generally associated with higher velocity static pressure.
- The pressure surface (lower surface) has a comparatively higher static pressure than the suction surface.
- Mean camber line: The locus of points halfway between the upper and lower surfaces as measured perpendicular to the mean camber line.
- Leading & trailing edges: The most forward and rearward points of the mean camber line.

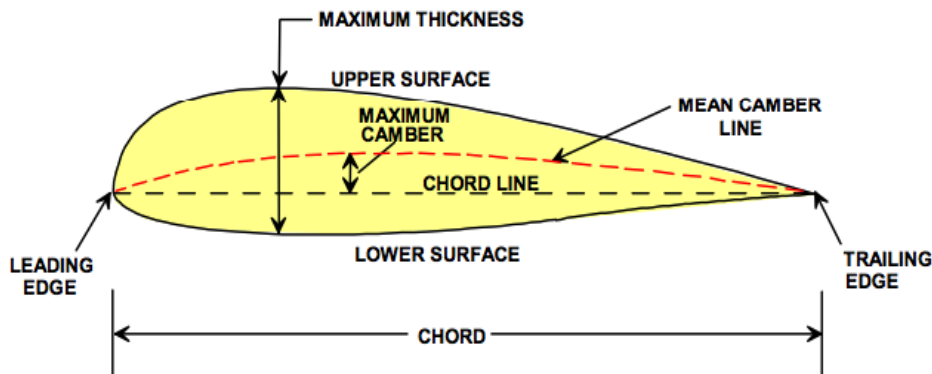


Figure.1.3 Airfoil shape

- Chord line: The straight line connecting the leading and trailing edges.
Chord C : The distance from the leading to trailing edge measured along the chord line.
- Camber: The maximum distance between the mean camber line and the chord line.
- Leading edge radius and its shape through the leading.
- The thickness distribution: The distance from the upper surface to the lower surface, measured perpendicular to the chord line.

1.1.2.Types of Airfoils

- The symmetrical aerofoil is distinguished by having identical upper and lower surfaces. The mean camber line and chord line are the same on a symmetrical aerofoil
- The non symmetrical aerofoil has different upper and lower surfaces, with a greater curvature of the aerofoil above the chord line than below. The mean camber line and chord line are different.

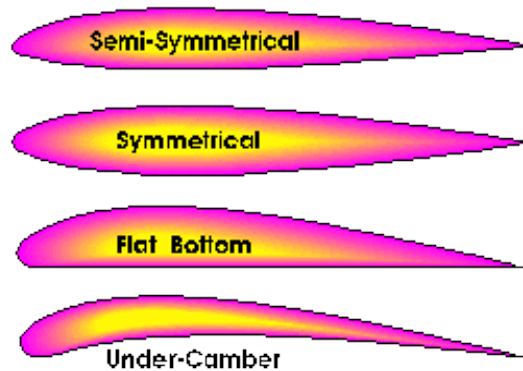


Figure.1.4. Types of airfoil

1.1.3. Airfoil series

- NACA (National Advisory Committee for Aeronautics) or NASA (National Aeronautics and Space administration) identified different airfoil shapes with a logical numbering system.
- NACA Airfoil Series
 - 1- NACA 4-digit series
 - 2- NACA 5-digit series
 - 3- NACA 1-series or 16-series
 - 4- NACA 6- series
 - 5- NACA 7- series
 - 6- NACA 8- series
 - 4- NACA 4- digit series
 - The NACA four-digit wing sections define the profile by
 - First digit describing maximum camber as percentage of the chord.
 - Second digit describing the distance of maximum camber from the aerofoil leading edge in tens of percent of the chord.
 - Last two digits describing maximum thickness of the aerofoil as percent of the chord.
 - Example: NACA 2412

NACA0012 Airfoil

We have chosen NACA0012 airfoil in the project.

Max thickness-12% at 30% chord.

Max. camber 0% at 0% chord.

Literature Review

1. Osama kandil., Bedriyagiz., Volkan Pehlivanoglu Y., (2011) “Drag minimization using active and passive flow control techniques”. The objective of this paper is to reduce the wave drag in transonic flight using flow control devices. most importantly, 3.94% decrease in the total drag and 5.03% increase in lift.
2. Mahe”, r Ben Chiekh., Mohsen Ferchichi., (2010) Jean- christophebera., “Modified flapping jet for increased jet spreading using synthetic jet”. It is an experimental investigation, using PIV system, the objective was to determine the optimal forcing conditions that would in jet spreading in a simple flapped jet.
3. E Montazer, E Salami, And S N Kazi, (October 2016) “Optimization of a synthetic jet actuator for flow control around an airfoil”. This paper deals with the optimization of a synthetic jet actuator parameters in the control flow around the naca0015 airfoil at two angle of attack. The results showed that the actuator is more effective for post angle of attack that can lead to an enhancement of 66% in L/D.
4. Deng, Xiong, Wang, Linluo, (June 2014) “A novel optimal design for an application oriented synthetic jet actuator”. This Paper presents a novel approach to the optimal design of an SJA applied to enhance fuel and air mixture. the result indicate that the optimal value of the strength of vortex pairs increases by 32.5% over the experimental data and more than 8.4% compared with the simulation results of the orthogonal experiments.
5. Lopez Mejia, O. D.,(2009) “Computational study of a NACA4415 airfoil using synthetic jet control”. This study is part of the avocet (adaptive vorticity control enabled flight) project and is intended to provide computational support for the design and evaluation of closed loop flow control with synthetic jet actuator for small scale UAV’S.
6. Zhao, Q. J., Ma Y. Y., and Zhao, G. Q., (2017) “Parametric analyses on dynamic stall control of rotor airfoil via synthetic jet)”. The effects of synthetic jet control on unsteady dynamic stall over rotor airfoil are investigated numerically. The results indicates that synthetic jet has the capability in improving aerodynamic characteristics of rotor.
7. Grzegorz Filip., Kelvin Maki., Peter Bachant., (2018) “Simulation of flow control device in support vehicle drag reduction”. The flow control device can enable vehicle drag reduction through the mitigation of separation and by modified local and global flow features that can designed to re-energized weakly attached boundary layers to prevent are minimize separation region that can increase drag.
8. Glezer, A., Amitay, M.,(2002). “Synthetic jets”. Annu. Rev. Fluid Mech. The paper discusses the formation and evolution of finite span synthetic jets and their applications for performance enhancement of fluid and thermal systems. Using synthetic jets can showed comparable effects to those of conventional ailerons at moderate deflection angles.

9. D. P. Rizzetta., M. R. Visbal., and M. J. Stanek.,(1999) “Numerical investigation of synthetic-jet flow fields,” The flow fields surrounding a synthetic jet actuating device are investigated numerically by direct simulation. The interior results are generated on an overset deforming zonal mesh system, whereas the jet flow field is obtained by a high order compact difference scheme.

10. Samimy, M., Kim, J.H., Kastner, J., Adamovich, I., Utkin, Y., (2007). “Active control of high-speed and high- Reynolds-number jets using plasma actuators”. Localized arc filaments plasma actuators are used to control an axisymmetric mach 1.3 ideally expanded jet of 2.54cm exit diameter and a Reynolds number based on the nozzle exit diameter of about 1.1×10^6 .

METHODOLOGY

In methodology, The flow separation over the symmetrical airfoil can be delayed by using synthetic jet actuator. There are two methods we are using to find the lift-to-drag ratio in symmetric airfoil. They are

- Numerical validation
- Computational fluid Dynamics

3.1. Steps involved in methodology

Increased numerical power and improved algorithms will also be necessary to improve CFD capability to accurately model the entirety of synthetic jet complex time dependent flows. Numerical models that included large eddy simulation (LES), reduced order models, 2D blended RANS-LES, laminar Navier Stokes and unsteady Reynolds Average Navier-Stokes (RANS). Most of the numerical cases were 2D with a few 3D models.

Computational Fluid Dynamic

Computational fluid dynamics (CFD) is a branch of CAE that simulates fluid motion and heat transfer using numerical approaches CFD software can analyse a range of problems related to laminar and turbulent flows, incompressible and compressible flow, multiphase flows and more.

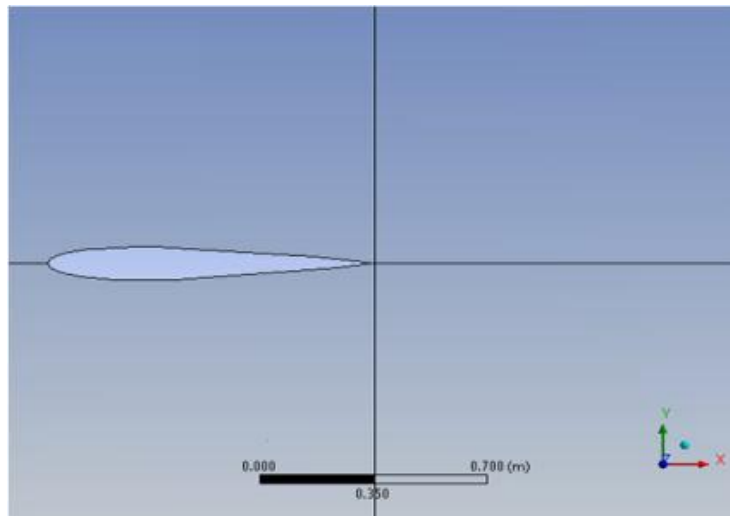


Figure 3.1: NACA0012 airfoil simulation

Numerical validation

For the purposes of this validation, the definition of the NACA 0012 airfoil is slightly altered from the original definition so that the airfoil closes at chord=1 with a sharp trailing edge. To do this, the exact NACA 0012 formula

$$y = \pm 0.6 * [0.2969 * \sqrt{x} - 0.1260 * x - 0.3516 * x^2 + 0.2843 * x^3 - 0.1015 * x^4]$$

is used to create an airfoil between $x=0$ and $x=1.008930411365$ (the T.E. is sharp at this location). Then the airfoil is scaled down by 1.008930411365 . Thus, the resulting airfoil is a perfect scaled copy of the 0012, with maximum thickness of approximately 11.894% relative to its chord (the original NACA 0012 has a maximum thickness of 12% relative to its blunted chord, but it, too, has a maximum thickness of 11.894% relative to its chord extended to 1.008930411365). The revised definition is:

$$y = \pm 0.594689181 * [0.298222773 * \sqrt{x} - 0.127125232 * x - 0.357907906 * x^2 + 0.291984971 * x^3 - 0.105174606 * x^4]$$

The turbulent NACA 0012 airfoil case should be run at essentially incompressible conditions (the recommendation here is to run $M = 0.15$ in compressible CFD codes). The Reynolds number per chord is $Re = 6$ million. Boundary layers should be fully turbulent over most of the airfoil. Inflow conditions for the turbulence variables should be reported.

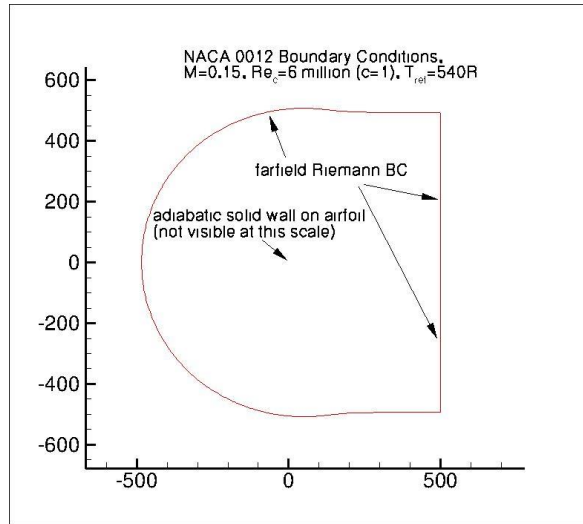


Figure 4.1: NACA 0012 boundary conditions

4.1 Boundary condition

The incoming flow velocity is $U_\infty = 27.38$ m/s specified at the inlet, with Reynolds number $Re = 19106$ based on the chord length c . At the outlet, static pressure is given. For the turbulence condition, a turbulence intensity (ratio of the fluctuating part to the mean velocity) of 5% is set at the inlet, together with a viscosity ratio (ratio of the turbulence viscosity to dynamic viscosity) of 10. In addition, an SJA that is shown in figure 1 is employed on the aerofoil for the flow control. The jet hole in a width of $1\%c$ is placed on the upper surface of the aerofoil, with a distance of $12\%c$ to the aerofoil leading edge. The initial parameters of the SJ are selected based on Refs. [23, 24], and will be optimized later. The jet frequency is set to be $f = 75$ Hz, and the angle between the jet flow and the tangential direction of the aerofoil upper surface is $\theta = 30^\circ$. The periodic velocity V_{jet} is introduced at the jet hole according to Eq. (1), with a maximum value of $V_{max} = 2.25U_\infty$. Furthermore, the lift and drag coefficients C_L and C_D are defined in Eqs. (2) and (3), respectively. The pressure coefficient C_p is also specified in Eq. (4):

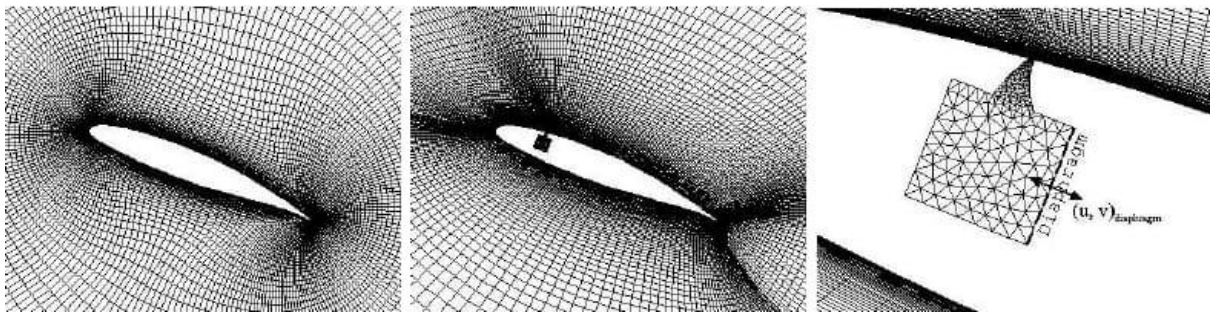


Figure 4.2: View of Computational grid

$$V_{jet}(t) = V_{max} \cdot \sin(2\pi ft) \tag{1}$$

$$C_L = F_L / (0.5 \rho c U_\infty^2) \tag{2}$$

$$C_D = F_D / (0.5 \rho c U_\infty^2) \tag{3}$$

$$C_p = (P - P_o) / (0.5 \rho U^2 \infty) \quad (4)$$

The CFD code ANSYS is used to solve the unsteady N-S equations. The SST turbulence model [25] is chosen to simulate the turbulent flow, which is a combination of k-x model near wall boundary and k-e model for the main flow. This model is assumed to be able to accurately predict the onset and amount of flow separations under the condition of adverse pressure gradients by including the transport effects into the formulation of the eddy viscosity. The second-order backward Euler scheme is chosen for the time term, the second-order format is applied for the discretization in space and other terms. In order to validate the applied numerical method, the predicted lift and drag coefficients are compared with experimental data provided by Somers, for the case without applying flow control.

Table 4.1: Parameters of NACA0012

Parameters	Values
Incoming flow velocity	U=27.38 m/s
Reynolds number	1×10^6
Angle of attack	$\alpha = 12^\circ$
Frequency	F=75Hz
Maximum velocity	2.25U

In addition, the CFD results are presented for both the SST and k-e models for comparison. It can be observed that the predicted lift and drag coefficients with the SST turbulence model agree generally well with experimental ones. Although some discrepancies are observed in the drag coefficient at high angle of attack between CFD and experimental results, the variation trends with the angle of attack are basically similar. Therefore, the applied CFD method with the SST model has been validated.

Table 4.2: Numerical values of lift-to-drag ratio

CASE	AOA=12°
With SJA	21.864
Without SJA	28.244

Simulation Outcomes

6.1. Pressure contour

From the figure 6.1 and 6.2 of pressure contours it can be seen the upper surface having lower pressure and the lower surface having higher pressure. This situation shows that pressure on lower side tries to lift the body and hence increases the lift coefficient. In the given figure of pressure contours it is shown that at the leading edge of the upper side there is a greenish colour and on the lower side the colour is reddish. Where red colour indicates a higher value of pressure and greenish colour indicates a lower value. As the angle of attack

increases the coefficient of lift also increases, but with the synthetic jet actuator at the same angle of attack the coefficient of lift increases.

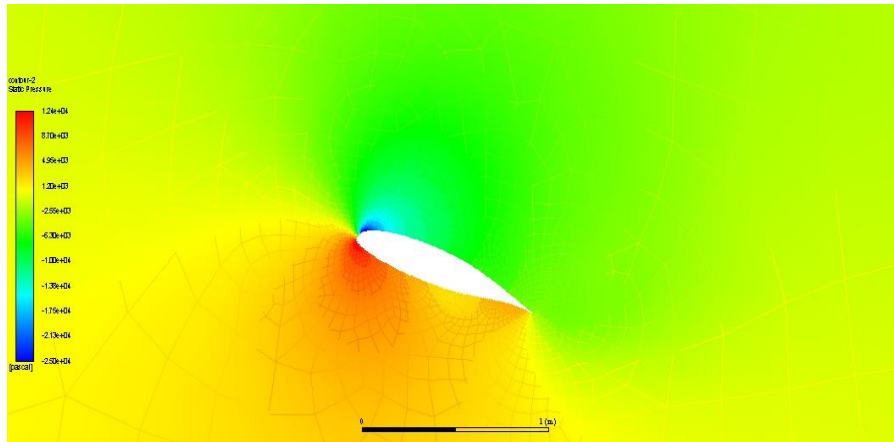


Figure 6.1: pressure contour without SJA

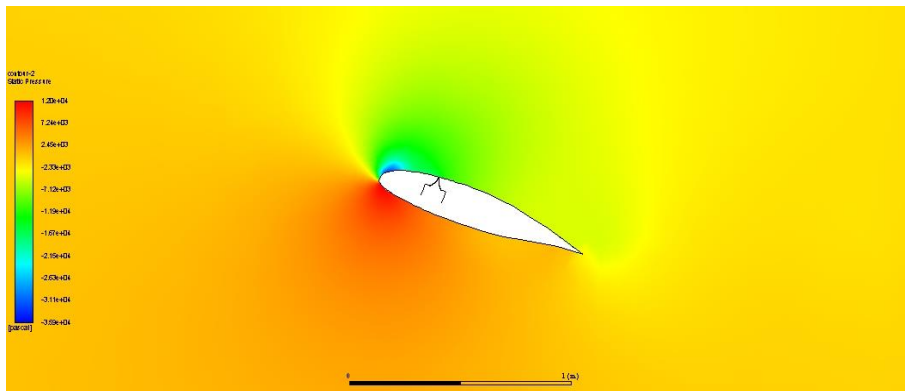


Figure 6.2: pressure contour with SJA

6.2. Velocity contour

The same thing can be seen in velocity contours that the upper surface of the airfoil in the figures 6.3 and 6.4 are shown in a reddish colour while lower surface is shown in bluish colour where a reddish colour indicates higher velocity and according to Bernoulli's Theorem it will have a lower pressure. Near the trailing edge there is huge gap amongst the velocity vectors which means that flow starts to separate near the trailing edge.

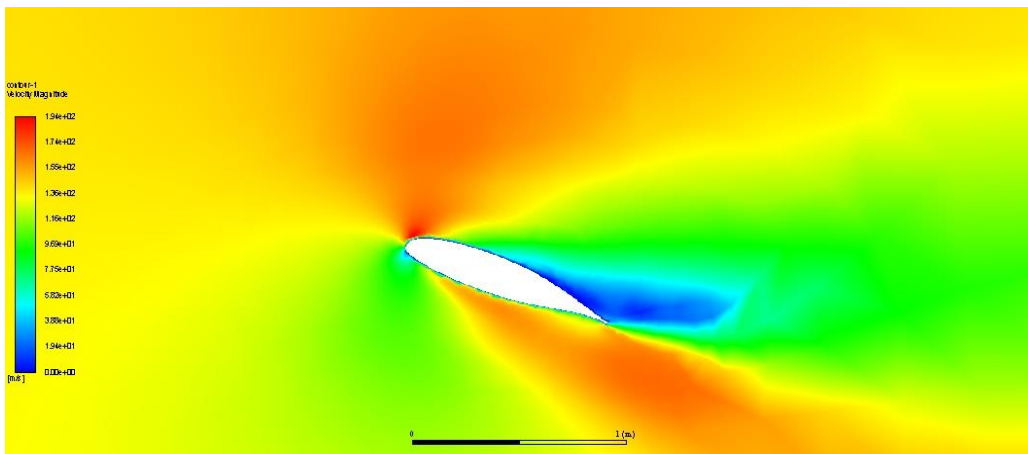


Figure 6.3: velocity profile at 12° angle of attack without SJA

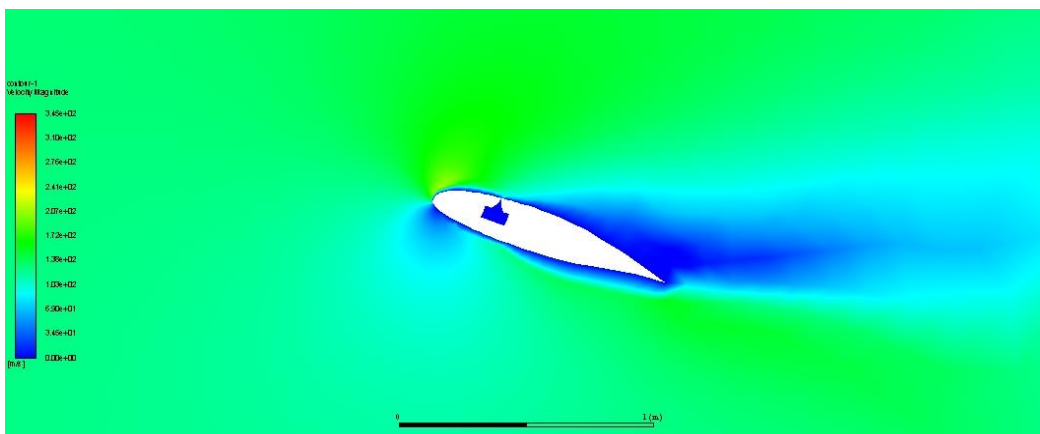


Figure 6.4: Velocity profile at 12° angle of attack with SJA.

6.3. Streamline contour

The pathlines are linear in figure 6.5 and the pathlines are turbulent in figure 6.6. The pathlines are linear when the airfoil is not attached with synthetic jet actuator. Meanwhile, figure 6.6 shows that the pathlines are turbulent because the airfoil is attached with synthetic jet actuator.

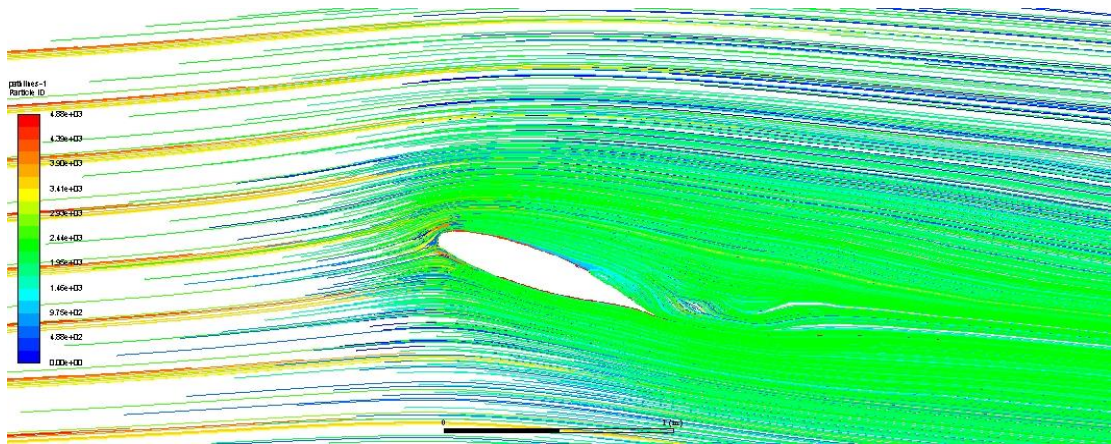


Figure 6.5: Pathlines at 12° angle of attack without SJA

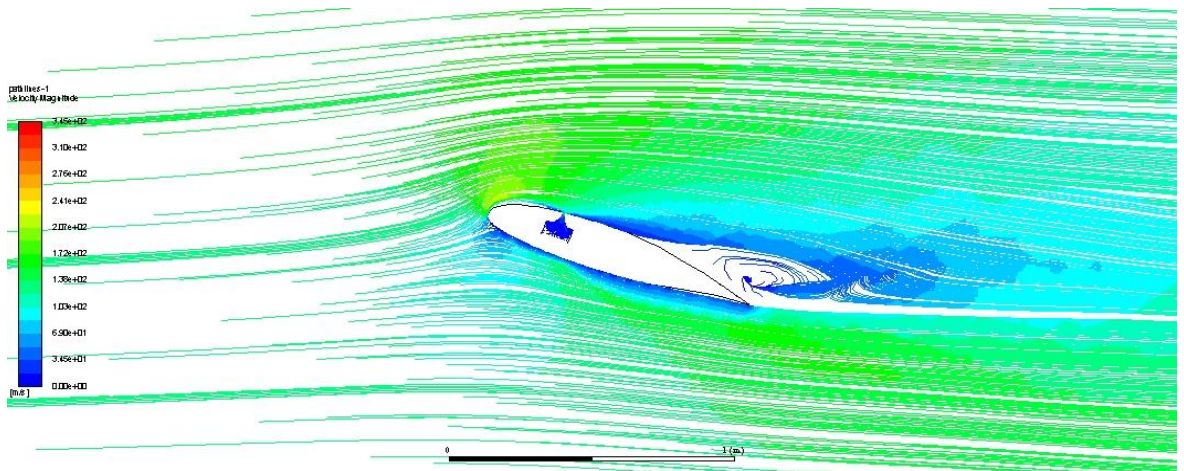


Figure 6.6: Pathlines at 12° angle of attack with SJA

Result and Discussion

The Coefficient of lift increases with the angle of attack increases. At certain angle of attack the stall condition is occurred so the generation of lift will be reduced. The comparison of the NACA0012 Airfoil with and without synthetic jet actuator. The lift to drag ratio of with and without synthetic jet actuator in an airfoil. The result has been shown below.

Table.7.1: The optimal result of NACA0012 airfoil with & without SJA

S.NO	CASE	AOA	Length of slot (mm)	Frequency (Hz)	Numerical value	Computational value
1.	Without SJA	12°	0.3	75	27.254	27.157
2.	With SJA	12°	0.3	75	28.149	28.544

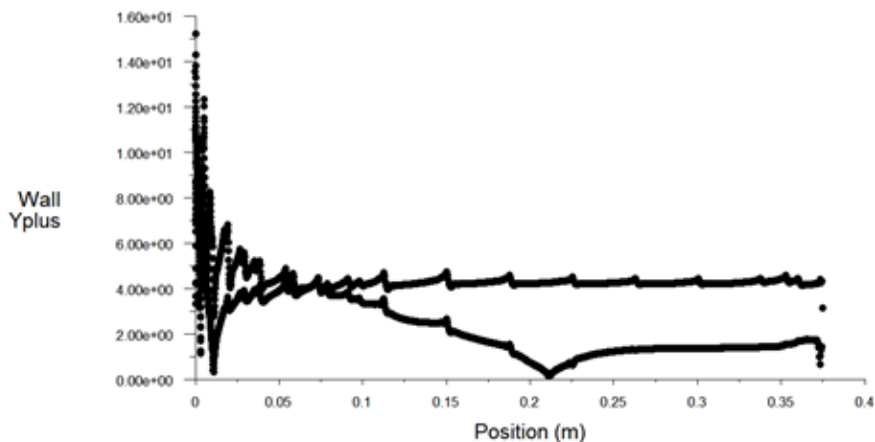


Figure7.1: Y+ on the airfoil surface with & without SJA

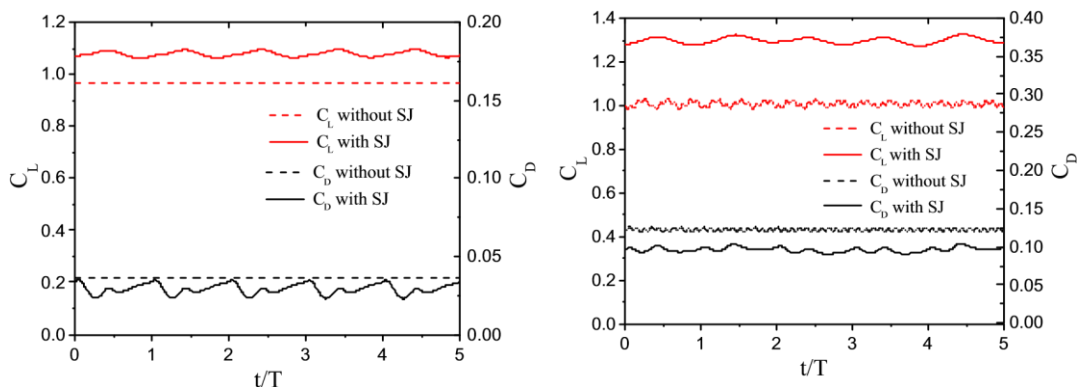


Figure7.2: Comparison of Lift-to-Drag ratio in NACA0012 airfoil.

Conclusion

The simulation of aerodynamics active control using synthetic jet actuator was performed, solving unsteady Reynolds-Averaged Navier-Stokes equations for NACA 0012 airfoil at Reynolds number, $Re = 896000$. The flow solver was coupled with the response surface methodology to optimize the jet performance in order to improve the aerodynamic characteristic of the airfoil. The optimization was performed for two angles of attack, i.e. stall and post stall angles of attack. Aerodynamic performance (L/D) was increased by 29% in stall angle of attack and the stall delayed from 13° . Meanwhile, in the post stall angle of attack, L/D had 66% improvement due to reattachment of the recirculation zone on the suction side of the airfoil. The optimum length of the synthetic jet slot was detected to be decreasing as the angle of attack increases. When the angle of attack increased the optimum synthetic jet location was moving to the leading edge. The location of the separation point moved toward the trailing edge on the upper surface as the synthetic jet actuator was used. The optimum actuation jet frequency and the jet outlet velocity observed to be decreasing as the angle of attack increased..

Obviously, the synthetic jet was indicated to be the most effective at post-stall angles of attack. It improved L/D significantly and postponed the flow separation.

References

1. Osama kandil., Bedriyagiz., Volkan Pehlivanoglu,Y., “Drag minimization using active and passive flow control techniques”,Aerospace science and technology(2011).
2. Maher Ben Chiekh., Mohsen Ferchichi., Jean-christophebera., “Modified flapping jet for increased jet spreading using synthetic jet”,International journal of heat and fluid flow(2010).
3. Amitay, M., Smith, B.L., Glezer, A., “Aerodynamic flow control using synthetic jet technology”AIAA paper No.98-0208 (1998)
4. Suzuki, T., “Effects of a synthetic jet acting on a separated flow over a hump”. Journal of Fluid Mechanics- 547, 331-359.
5. Zhang, P.F., Wang, J.J., Feng L.H., “Review of zero-net-mass-flux jet and its application in separation control”. ASME journal of fluid engineering. 128, 1053-1062(2006).
6. Zheng, X., Zhou, S., Hou, A., Jiang, Z., Ling. D., “Separation control using synthetic vortex generator jets in axial compressor cascade”, Acta Mech. Sin.22, 521-527(2006)
7. Lopez Mejia, O. D., 2009 “Computational study of a NACA4415 airfoil using synthetic jet control”PhD Thesis University of Texas at Austin.
8. Zhao, Q. J., Ma Y. Y., and Zhao, G. Q., 2017 “Parametric analyses on dynamic stall control of rotor airfoil via synthetic jet”.Chinese Journal of Aeronautics 30(6): 1818–1834.
9. Herliah, A., Baso, Y. S., Hidayanty, H., Syarif, S., Aminuddin, A., & Bahar, B. (2022). Effect of web-based she smart education models on adolescent girl’s knowledge, attitudes, and practice about obesity. International Journal of Health & Medical Sciences, 5(1), 50-55. <https://doi.org/10.21744/ijhms.v5n1.1832>
10. Samimy, M., Kim, J.H., Kastner, J., Adamovich, I., Utkin, Y., 2007. “Active control of high-speed and high-Reynolds-number jets using plasma actuators”.Journal of fluid Mechanics.578,305-330.
11. Zhang, P.F., and Wang, J. J., 2008. “Numerical simulation on flow control of stalled NACA0015 airfoil with synthetic jet actuator in recirculation region”. Journal of beijing sadhana (2019)44:190 page 9 of 10 University of Aeronautics and Astronautics 34(4):443– 446.
12. Glezer., M. Amitay., and A. M. Honohan., “Aspects of low and high-frequency actuation for aerodynamic flow control,”. *AIAA Journal*, vol. 43, no. 7, pp. 1501–1511, 2005.
13. Rinaritha, K., & Suryasa, W. (2017). Comparative study for better result on query suggestion of article searching with MySQL pattern matching and Jaccard similarity. In 2017 5th International Conference on Cyber and IT Service Management (CITSM) (pp. 1-4). IEEE.
14. Amitay, M., Smith, D.R., Kibens, V., Parekh, D.E., and Glezer, A., “Aerodynamic flow control over an unconditional airfoil using synthetic jet actuators”. AIAA journal, vol.39, no..3, pp.361-370, 2001.
15. Glezer, A., Amitay, M., 2002. “Synthetic jets”. Annu. Rev. Fluid Mech. 34, 503–529.

16. Graftieaux, L., Michard, M., Grosjean, N., 2001. "Combining PIV, POD and vortex identification algorithms for the study of unsteady turbulent swirling flows". *Meas. Sci. Technol.* 12, 1422-1429.